Experimental Investigation of Boron Combustion in Air-Augmented Rockets

K. Schadow*
Naval Weapons Center, China Lake, Calif.

Studies have been made using a windowed combustion tunnel to examine the mixing and burning between subsonic air and a supersonic fuel-rich exhaust of a rocket motor burning hydrogen-oxygen-boron mixtures. The reaction processes were recorded by high-speed cinephotography. Results of experiments are presented in which the following parameters were varied: 1) boron concentration in the propellant (up to 55% by weight), 2) nonequilibrium chamber temperature of the primary rocket (750°K to 2500°K), and 3) air to propellant flow ratio (3 to 15). The temperature of the primary rocket was calculated by assuming boron as a heat sink. These calculations showed good agreement with experimental data at low chamber temperatures. The strong influence of the primary nonequilibrium chamber temperature on the boron combustion efficiency was demonstrated using the results of particle sampling probes and c*-efficiency measurements. By increasing the chamber temperature from 750°K to 2000°K the over-all reaction efficiency was improved from 85 to 94%.

1. Introduction

THE development of air-breathing rockets is closely related to combustion studies of propellants heavily loaded with boron. From the standpoint of volumetric energy release it is desirable to maximize the metal content in the propellant of the primary rocket. However, the theoretical gain in specific impulse can be, of course, only attained with efficient boron combustion. This is an important factor in the analysis of air-augmented rockets because preliminary combustion tests have indicated that the boron combustion will not be initiated in the primary rocket chamber if one burns solid propellants containing 50% (by weight) boron, or more.[1]

The exact conditions for boron ignition and burning are not known. Data of Ref. 2 show that clean boron particles react spontaneously with air at temperatures of about 400°K. But according to Ref. 3, only a slow surface oxidation takes place at temperatures below the oxide melting point (720°K). A strong temperature dependence of the reaction rate was observed by the same author. When the temperature was increased to the region of the metal melting point (2300°K) and oxide boiling point (2326°K), a sharp increase in boron oxidation rate was noted. Prentice[4] made the same observation in preliminary tests, when burning single boron particles in air. Color pictures indicated that the temperature of the particle rose relatively slowly after the particle was exposed to a thermal energy source; this slow ignition phase was finally followed by vigorous particle combustion.

The first slow reaction phase at relative low temperatures does not appear to be desirable in an air-augmented system if one considers the relatively short residence times associated with rockets. The temperature for initiating vigorous burning is dependent on kinetic and physical conditions that are not yet known. Therefore, in thermodynamic calculations for systems consisting of fuel, oxidizer, and boron, in which the conditions for vigorous boron combustion are not reached, it is more meaningful to consider the boron in the fuel-oxidizer combustion matrix as an inert heat sink. The temperature produced by the combustion of the nonboron portion of the fuel and the oxidizer is called the nonequilibrium combustion temperature T^*. This temperature determines whether or not satisfactory ignition will occur in the combustion zone environment.[5] Cohen[6] presented some theoretical considerations on fuel-rich solid propellant heavily loaded with metals in air-breathing propulsion using the nonequilibrium combustion temperature.

This paper presents results of an experimental research program which has been started at the Naval Weapons Center to study the boron combustion behavior in ducted rockets. A test stand was built which permits the observation of the boron combustion in the afterburner with high-speed cinephotography. In this paper the results of experiments are presented, in which the following parameters have been varied: 1) boron concentration in the propellant, 2) nonequilibrium chamber temperature of the primary rocket, and 3) air to propellant ratio. The influence of the primary chamber temperature on the combustion efficiency was demonstrated by efficiency measurements and particle sampling probes behind the afterburner.

2. Experimental Apparatus

The major components of the test facility are: 1) air supply system, 2) combustion tunnel with primary rocket, 3) propellant feed system for the primary rocket, 4) optical system for direct high-speed photography and schlieren photography, 5) device for particle sampling, 6) electronic equipment for efficiency measurement, and 7) timer system for remote control of ignition, flow valves, photography, and particle sampling.

2.1 Air Supply System

The main components of the air supply system are a 240-ft^3 air reservoir capable of storing air at 2500 psi, a flow control system with an orifice meter for flow meas-

Presented as Paper 68-634 at the AIAA 4th Propulsion Joint Specialist Conference, Cleveland, Ohio, June 10–14, 1968; submitted June 19, 1968; revision received April 21, 1969. This work was performed under Naval Ordnance Systems Command ORDTASK ORD-033-123/200/F009-06-05, and NWC Independent Research funds, and under Fellowship of Bundesministerium für Wissenschaftliche Forschung, BRD. The author wishes to express his appreciation for the helpful discussions with J. E. Crump and J. Prentice, and the support of A. Ballew in running the experiments. The test facility was planned and designed by R. Slates (deceased).

* Scientist Exchange Fellow, Aerothermo-chemistry Division, Research Department; presently Head, Liquid Propulsion Systems Branch, Division for Chemical Rocket Propulsion, Jet Propulsion Department–Deutsche Forschungsanstalt für Luft- und Raumfahrt.

urement, and an air preheater which burns liquid alcohol directly with the high-pressure air passing through the burner. The specifications of the air preheater are: $p_{max} = 1000$ psig, $T_{max} = 2000°F$, and $\dot{m}_{max} = 12$ lb/sec.

2.2 Combustion Tunnel with Primary Rocket

As shown in Fig. 1 the combustion tunnel is composed of four sections of square cross-sectional tubes. The air enters the tunnel from the left side through a choked throat, which makes the airflow independent from the pressure in the tunnel as long as the ratio of the pressure before and after the throat is larger than about two. In the tunnel the air is divided into two streams which pass the primary rocket on the top and on the bottom through two rectangular channels. Then the air enters the secondary combustion chamber where it mixes with the exhaust of the rocket. This reaction zone can be optically observed through four pairs of quartz windows mounted on opposite sides of the tunnel walls. Each quartz window allows a free viewing zone of 4 in. × 2.3 in. The reaction products leave the combustion tunnel through a throat with 3-in. diameter. The characteristic length of the secondary combustion chamber (L^*) based on the length from primary to secondary nozzle is 14.4 ft; the corresponding residence time based on a temperature of 2500°K is 4 msec.

The primary rocket and its feed system are similar to that described by Dean et al.[7] The hemispherical injector has four streams of oxygen gas impinging on a central fuel stream, which contains all of the boron powder and about 50% of the total hydrogen gas flow. The remaining hydrogen gas is injected through two orifices, placed in the rocket body about in the middle of the motor length. The parts of the rocket are made of copper, which allows a burning time of a few seconds without any external cooling.

The copper nozzle has a 0.480-in. throat diameter, and an expansion ratio of 2.68. The characteristic length (L^*) of the rocket is 83 in.; the corresponding residence time based on a temperature of 2500°K is 1.9 msec.

2.3 Propellant Feed System

Hydrogen and oxygen are supplied from standard high-pressure gas cylinders. After pressure reduction the flow rates are measured with orifice meters. The other control devices of the flow system are described in Fig. 1. The boron powder (Kawecki, with an average particle size of less than 1 μ) is transported to the burner by entraining it in the H_2 gas by means of a pneumatic transport system. The average boron powder flow rate is determined by weighing the powder reservoir before and after each test. The nonequilibrium chamber temperature of the primary rocket can be changed by varying the oxygen-hydrogen ratio. The boron mass flow is mainly dependent on mass flow of the carrier gas and the amount of powder filled into the reservoir, so that a variation is feasible within certain limits. For improved transport conditions the boron powder is mixed with a small amount of Cab-o-sil, a silica powder of about 0.01 μ particle size.

The rocket is ignited with a pyrotechnic igniter. After one second burning time with H_2 and O_2 only, boron is fed into the rocket for one second. After stopping the boron flow the rocket again burns only H_2 and O_2 for one second. It is found that the boron reaches steady-state combustion conditions very quickly so that the boron feed time can be limited to one second. During this time the boron flow rate is sufficiently constant.

2.4 Optical System

With the established test facility the boron combustion behavior can be investigated by various optical devices. During this work the afterburning behavior was recorded with a Hycam camera on Anscochrome D/200 color film at 2500 frames/sec. In addition, schlieren pictures were made of the reaction in the secondary chamber. The schlieren system was based on two lenses with a parallel light beam for the working section. The pictures were taken with a spark duration of about 2 μsec. The spark was triggered by a shutter of a camera without any lens. The exposure time of 10 msec given by the camera was short enough so that the schlieren picture was not overexposed by the combustion flame.

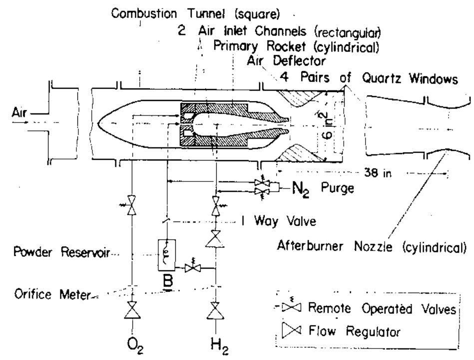

Fig. 1 Schematic diagram of combustion tunnel with primary rocket.

2.5 Particle Sampling Device

For a rough but instructive determination of the effectiveness of the boron particle combustion, a microscope glass plate fastened on a metal block was dropped in nearly free fall through the exhaust gases of the afterburner. The falling probe was guided in two tracks with sliding Teflon bearings. The contact time of the sampling device with the gas is determined by its weight, and the friction in the bearing due to the dynamic pressure.

2.6 Electronic Data Recording

During a run, measurement was made of the rocket motor chamber pressure; static pressure in the afterburner just upstream of the end of the constant area duct section; mass flow rate of oxygen, hydrogen and air; air stagnation temperature in the plenum of the duct downstream of the air entrance throat; air static pressure in rectangular channel on the top of the rocket; and rocket body temperature. The latter measurement was also used to trigger an emergency switch for rocket shutdown due to rocket body over-temperature. The operating of the primary rocket, as well as the photographical data recording and the particle sampling, were automatically controlled by a sequential timer.

3. Procedure of Color Picture Evaluation and Data Reduction

3.1 Color Picture Evaluation

In using a color picture for information about the boron combustion behavior it is necessary to determine the different colors which correspond to specific processes of the hydrogen-oxygen-boron reaction. If one studies the produced combustion species, only the molecular bands of the boron oxides and the continuous body radiation from the boron particles have to be considered. If the boron particles leave the primary rocket at very low temperature the changing color scale is visible during the heatup time of the particles in the secondary chamber. These colors recorded by photography can be roughly compared with the colors of a blackbody at different temperatures. The determination of the temperatures is only possible in certain limits, as shown in Fig. 2 (also see Table 1). A calibration of the sensitivity of the color film as a function of wavelength by taking photographs with a standard radiation source was not performed. The

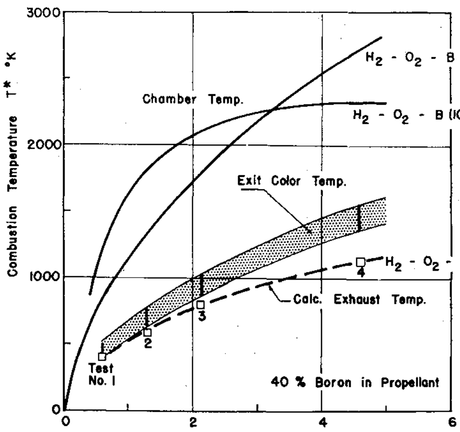

Fig. 2 Primary rocket temperatures.

correlation of the color scale and the true temperatures of the blackbody are taken from Ref. 8; see Table 2.

The true temperature of the particle is only slightly higher than its color temperature, as determined by the comparison with the blackbody color. The characteristic molecular emission of the boron oxides are the green bands of the species BO_2, an intermediate in the formation of B_2O_3. Therefore, the green color is a good indicator of boron combustion. The gaseous species B_2O_3 is colorless, whereas condensed B_2O_3 is white. The B_2O_3 should be in the gaseous phase in the afterburner flame if the temperature is above 2326°K (B_2O_3 boiling point) and condensed boron oxide should be noticed as a white vapor in the exhaust and on cooler parts of the test sections.

3.2 Combustion Efficiency and Temperature Calculation

For tests with various primary chamber temperatures the combustion efficiency of the hydrogen-oxygen-boron-air reaction has been calculated based on static chamber pressure in the secondary chamber. With this value of P_{CAF}, the total mass flow of the air ($\dot{m}_A$), the primary rocket propellant ($\dot{m}_{H+O+B}$), and the throat area A_t of the afterburning, the experimental characteristic velocity c^* for the combustion process can be calculated;

$$c^*_{\text{exp}} = \frac{P_{CAF} \cdot A_t \cdot g}{\dot{m}_{(O+H+B)} + \dot{m}_A} \text{ (fps)} \tag{1}$$

This experimental value was compared with the theoretical ideal characteristic velocity assuming complete mixing and combustion, as well as shifting equilibrium in the afterburner, and is discussed later.

It can be seen from Eqs. (1) that the processes in the primary rocket do not appear separately in the combustion efficiency calculation. Therefore, some calculations were made concerning the primary reaction. As shown in the Introduction the nonequilibrium temperature is an important parameter in a system with metal particles where the physical and kinetic conditions are such that the metal ignition requirements are not being reached. In this paper the nonequilibrium temperature for the primary chamber was computed for hydrogen-oxygen-boron mixtures. From these data the primary rocket exit temperature was calculated with the assumption of frozen equilibrium and ideal gas conditions in the nozzle. Crowe[9] showed that the particles can be considered in thermal equilibrium with the gaseous species so that the particle exit temperature can be determined.

3.3 Particle Sampling Evaluation

After each test the sampling probe was covered with a white layer and accumulations of quenched particles. No attempt was made to analyze chemically the residue on the sampling probe. Microscopical investigations showed that the white layer was transparent using backlight and was soluble in water. These are characteristic qualities of boron oxide. The same experiments showed that most of the sampled particles were unburned boron. Thus, the efficiency of the boron combustion of different tests can qualitatively be evaluated by comparing the amount of particle residue on the sample probes.

4. Results

4.1 Primary Rocket

Tests run without air flowing through the tunnel indicated that the color temperature of the particles at the exit of the primary rocket changed with varying chamber temperature. Figure 2 compares the recorded color temperatures with the computed chamber temperatures of the hydrogen-oxygen-boron mixture for 40% boron (by weight) as a function of the weight ratio of oxygen to hydrogen. The calculations were made for 100% and 0% boron reacting and are indicated with B (100) and B (0) respectively. The temperature for the B (0) reaction exceeds the temperature of the B (100) reaction at high O/H ratios. This is to be expected if one compares the heat of formation and heat of combustion of water [reaction product for B (0)] and boron oxide [reaction product for B (100)].

The calculation with 100% boron reacting is unrealistic at low O/H mixture ratios because the boron particles will not achieve satisfactory ignition in the hydrogen-oxygen combustion zone. The exhaust temperature of the reaction products was calculated therefore with B (0) assuming frozen equilibrium and ideal gas conditions in the nozzle. The influence of boron concentrations higher than 40% on the calculated nonequilibrium chamber temperature will be shown later.

These computed temperatures were compared with the recorded color temperatures of tests 1 through 4 (for test data see Table 3, which summarizes the conditions of tests discussed in this paper). The boron concentration of these tests varied from 33% to 55%, so that the conditions of the theoretical program (40% B) are not entirely satisfied. Under these described conditions only moderate accuracy for the calculated and semiquantitative temperature determination can be expected. The color temperature is higher than the calculated temperature. This can be due to the fact that the particles being at relative high temperature in the chamber are not in thermal equilibrium with the expanding gases in the nozzle and/or that the particles are reacting. The chamber temperature had a strong influence on the boron deposit in the primary rocket nozzle. At chamber temperatures lower than about 1300°K and higher than about 2000°K no deposit was observed in the nozzle after the tests. Between these temperatures a layer up to 0.6 mm thick of agglomerated boron was noticed in the divergent part of the nozzle.

4.2 Secondary Combustion of Gaseous Species

From the previous discussion it can be seen that satisfactory boron ignition is not achieved in the primary rocket

Table 1 Primary rocket temperatures

Test results	Test 1	Test 2	Test 3	Test 4
Particle color	No radiation	No radiation	Dark	Yellowish
Radiation at nozzle exit	(No radiation from rocket inside)	(Red from rocket inside)	Red	Red to white
% Boron in prop	55.2	39.2	46.2	33

chamber at low temperatures. Thus the temperature for this process has to be supplied by the reaction of the gaseous species expelled from the rocket with the air and/or from the beginning oxidation of the boron particles with the ingested air. As discussed in the Introduction, the reaction rate of the boron oxidation is slow at low temperatures, although spontaneous reaction between boron and air does occur at these temperatures. The conditions for this reaction are favorable when the boron expelled from the primary rocket has a clean surface and most of the oxide has been dissolved in the water vapor of the hydrogen-oxygen reaction; nevertheless, the energy release of the beginning boron oxidation at these low temperatures should be less than the energy release of the hydrogen-air reaction by a considerable factor. This reaction can supply the energy for heating up the boron particles within a sufficiently short secondary chamber length to a temperature where satisfactory ignition should be achieved. Neglecting the oxidation energy of the boron particle, the temperature for the hydrogen-air reaction with boron as a heat sink can be calculated.

In this calculation it is assumed a priori that hydrogen and oxygen (of the air) react at any temperature. But, as known, the lowest ignition temperature of hydrogen in air is about 850°K. On the other hand, the tests showed that in the start phase of each test (with hydrogen-oxygen and air only), an afterburning of the hydrogen occurred with the air in the secondary chamber at temperatures where the hydrogen could not possibly ignite without a flame holder. The following are possible explanations for this apparent discrepancy:

1) possibility of free radicals in the primary exhaust reducing the ignition temperature of the hydrogen;

2) small amount of boron particles (from the preceding test) in the primary exhaust, which react spontaneously with the air. The reaction initiates the hydrogen ignition;

3) catalytic effect of the boron particles (from the preceding test) in the primary exhaust, which diminishes the ignition temperature of the hydrogen in the air.

From the preceding discussion it can be seen that two processes for initiating satisfactory boron combustion are important: 1) beginning boron oxidation, and 2) secondary combustion of the hydrogen in the air. The energy release of the first process is unknown. The nonequilibrium temperature of the second process was calculated with boron (as a heat sink) as a function of the air to propellant ratio, assuming complete mixing and combustion. The specific conditions for this calculation are summarized in the Discussion section. From the theoretical standpoint the reaction products can heat the boron particles up to 2300°K under advantageous conditions.

From the standpoint of boron combustion efficiency it is also important to achieve a quick ignition in order to burn the boron particles in the secondary chamber within a minimum length. Therefore, it is important to have efficient mixing and combustion of the gaseous rocket species with the air. This was studied using the schlieren technique and the results are shown in Fig. 3. Altogether six tests were run for this figure. Tests 5, 6, and 7 (as well as tests 8, 9, and 10) were made under the same conditions; the schlieren pictures were taken at different windows. The pictures from tests 8–10 were made under the conditions similar to test 1,

Table 2 Correlation of color scale and tree temperature of blackbody

Color	T°K
Incipient red heat	770–820
Dark red heat	920–1020
Bright red heat	1120–1220
Yellowish red heat	1320–1420
Incipient white heat	1520–1620
White heat	1720–1820, and higher

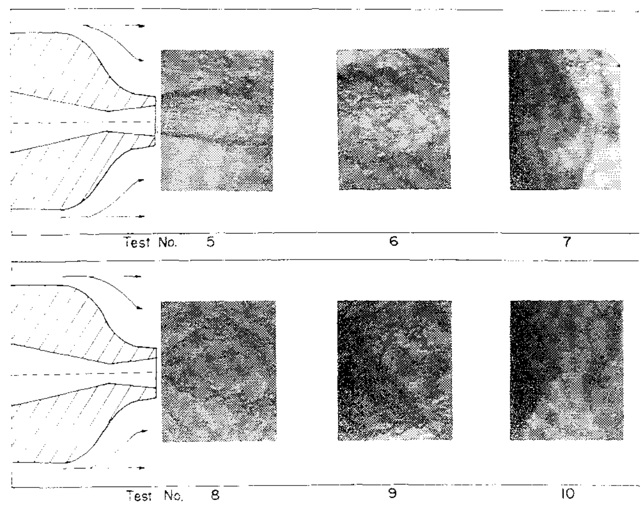

Fig. 3 Differences in the mixing and combustion characteristics changing the unreacted amount of hydrogen in the rocket (mole H_2/mole gas) primary: 0.68 (test 5–7), 0.94 (test 8–10).

with a low chamber temperature (see Fig. 2) and a high hydrogen mole concentration in the exhaust products. The mole hydrogen to mole gas ratio in primary rocket was 0.94. The picture of tests 8–10 shows that under these conditions a strong mixing and afterburning occurs behind the nozzle exit (test 8). In the second window (test 9) a more definite, expanding reaction front can be noticed. The reaction front reaches the chamber wall at the place of the third window (test 10), so that complete mixing and combustion of the hydrogen and the air can be assumed downstream of this chamber length. With the specific test data of tests 8–10 (see Table 3) complete mixing was reached at a distance of 10 D_e behind the primary nozzle exit in a secondary chamber of $D = 7.4 D_e$. (D_e = nozzle exit diameter of primary nozzle.) The mixing and combustion characteristic at a lower mole hydrogen to mole gas ratio (0.68) in the primary rocket is shown in Fig. 3 (tests 5–7).

It was found that the temperature of the ingested air has no influence on the ignition and combustion behavior of boron under the conditions tested in this program. The air temperature was varied from 280°K to 700°K, which is the approximate value for simulated flight conditions. This indicates that the hydrogen-air reaction temperature exceeds the air temperature of 700°K by a considerable factor.

4.3 Boron Combustion in Secondary Chamber

The evaluation of the high-speed movies indicated that the combustion in the secondary chamber was turbulent at high hydrogen mole concentration in the primary rocket and that the shape of the reaction plume fluctuated. However, the typical color of each run did not change with the burning time, so that the boron combustion behavior can be discussed using one representative picture of the film. Results of tests are presented in which the following parameters were changed: 1) percentage of boron in propellant, 2) nonequilibrium primary chamber temperature, and 3) air to propellant ratio.

4.3.1 Percentage of boron in propellant

The influence of the amount of boron in the propellant on the combustion behavior was demonstrated under test conditions explained in Fig. 4. Burning a relatively small percentage of boron in the primary rocket (test 11), there was no visible emission near the nozzle exit area. After a certain distance two green mixing regions were seen on the top and the bottom of the exhaust. The green color indicated the

Table 3 Test conditions

Test number	Total propellant flow, $\dot{m}$ kg/sec	% Boron in propellant	Oxygen/hydrogen ratio by wt	Air temp T_A, °K	Air/propellant ratio by wt	Primary chamber, psia	Secondary pressure, psia	Primary chamber temp T^*, °K
1	0.087	55.2	0.61	280	6.7	95	26.5	750
2	0.123	39.2	1.29	...	...	272	...	1320
3	0.121	46.2	2.12	...	...	263	...	1760
4	0.138	33	4.58	...	...	340	...	2720
5-6-7	~0.131	~33	2.3	280	~3.6	~318	~29.1	1650
8-9-10	~0.086	~55	0.6	280	~6.5	~94	~26.4	750
11	0.077	8	2.25	650	10.7	232	30.9	1850
12	0.098	31	1.95	650	12	241	40.9	1700
13	0.135	32.6	2.34	280	3.6	320	29.4	2000
14	0.108	32	1.81	280	5.1	260	28.6	1600
15	0.109	33	1.82	280	11.8	262	56.0	1600
16	0.088	51.3	0.5	280	15.5	108	48.9	750
17	0.105	41.9	1.16	280	5.5	167	28.1	1250
18	0.109	33	1.82	280	5.0	263	28.7	1650

presence of BO_2. Both mixing regions spread into the airstream, as well as to the centerline of the plume forming a wedge shape contour with almost no color radiation. The green of the mixing zone became brighter with the mixing length. In the fourth window, strong, brilliant white-green radiation could be observed only in the outer regions of the jet, indicating insufficient oxygen in the center of the plume.

Figure 4 (test 12) shows the results of a test under similar conditions, but burning 31%. The boron particles left the primary rocket at red color temperature, which turned rapidly to yellowish-red. The green in the mixing regions was more intense than in test 11, and the change to brilliant white-green could be noticed farther upstream (in the second window). The intensity continued to increase with increasing mixing length. Obviously, it was not difficult to burn high boron concentrations under these specific conditions. The temperature rise of the particle cloud from its red glow to intensive white-green was established after a mixing length of about 3 D_e (D_e-nozzle exit diameter of primary nozzle) in the outer regions of the jet, so that the burning of high boron concentrations in comparison to lower concentrations was limited only by the mixing efficiency of the air flow and the exhaust plume.

4.3.2 Primary chamber temperature

Figure 5 shows the boron combustion behavior at two different primary chamber nonequilibrium temperatures. In both tests the mass flow rates of hydrogen, boron, and air were kept almost constant, whereas the oxygen mass flow rate in test 1 was higher than in test 13; thus, the nonequilibrium chamber temperature was increased from about 750°K to about 2000°K. With increasing oxygen mass flow the propellant weight increases, so that the characteristic parameters related to the propellant weight (air to propellant ratio, percent boron in propellant) changed, although the air and boron mass flow rates were constant. For specific test conditions see Table 3. As discussed earlier, the particles in test 1 left the primary rocket showing no radiation. As the particle temperature increased, the entire heat color scale from dark red to bright yellow was observed over all the visible reaction zone. In the third and fourth windows green color indicated boron combustion on the outer boundaries of the reaction plume. This showed that the energy generation from the hydrogen-air reaction and from the slow surface oxidation of boron went into heating the boron particles. Boron combustion occurred only on the jet boundaries near the hydrogen-oxygen combustion zone and in regions with large oxygen excess. Where these conditions were not established (plume center) the color temperature of the particles was relatively low.

This boron reaction behavior, indicative of very poor combustion, changed entirely at the higher chamber temperature. The particles were expelled from the rocket with red radiation and the boron combustion started immediately when the exhaust was mixed with the air. The green mixing

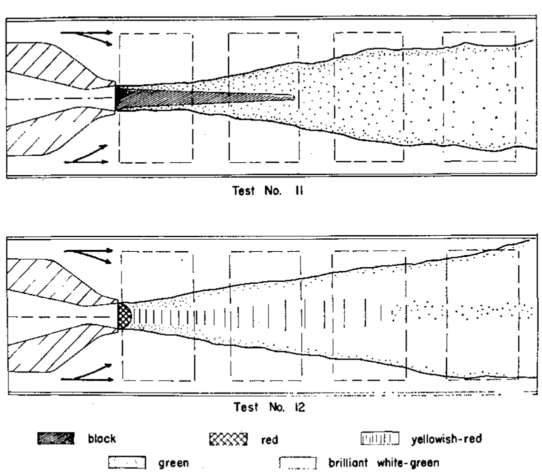

Fig. 4 Boron combustion behavior at different boron concentrations in the propellant. Test 11: 8% by wt, test 12: 31%.

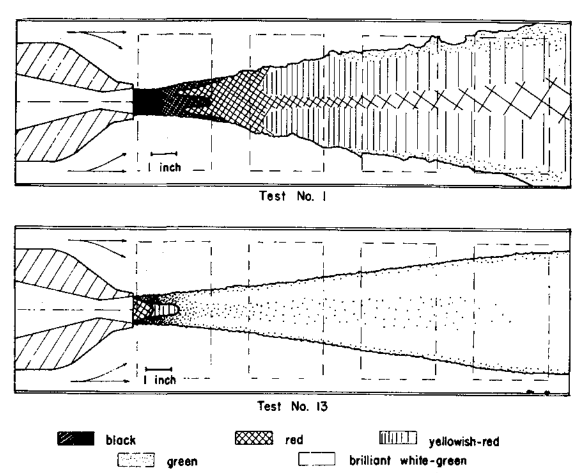

Fig. 5 Boron combustion behavior at different nonequilibrium primary combustion temperatures. Test 1: 750°K, test 13: 2000°K.

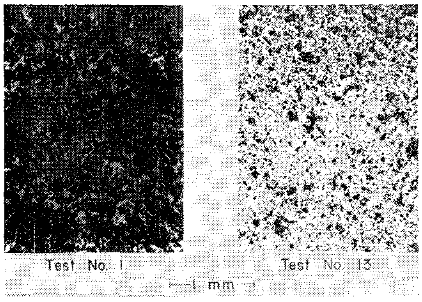

Fig. 6 Particle sampling probes at different nonequilibrium primary rocket combustion temperatures. Test 1: 750 K, test 13: 2000° K.

and combustion zone spread very fast to the center of the jet, so that after a mixing length of about 1.5 D_e the entire reaction zone was green. At the outer regions of the jet this green changed to brilliant white-green with the intensity increasing with increasing mixing length. It is not yet known whether the brilliant white-green was a very intense green band of BO_2 or a superimposition of the green BO_2 emission with the white color temperature of the reacting particles at a very high temperature.

The improvement of the boron combustion behavior with primary chamber temperature has been confirmed by particle sampling probes behind the afterburner nozzle. The probes (1 in. × 3 in.) showed both the quenched boron particles and condensed B_2O_3. The density of the boron particle accumulation changed at different locations on the glass plate depending on their position in the exhaust jet. The density was greatest in the jet center. Two microscope magnifications of these areas are shown in Fig. 6, comparing the results for test 1 and test 13. The pictures were made with transmitted light and show the B_2O_3 as white areas and the quenched particles as dark. The pictures indicated that the amount of boron burned was significantly higher at higher primary chamber temperature.

The qualitative but instructive results of tests 1 and 13 have been confirmed by c^*-efficiency determinations using Eq. (1). Figure 7 shows the influence of the chamber temperature on the experimental c^*-efficiency for four tests, in which the oxygen mass flow was increased from test 1 to test 13 keeping the mass flow of boron, hydrogen, and air almost constant (for test conditions see Table 3). The c^*-efficiency, including the hydrogen and boron combustion, as well as the mixing process of the air with reaction products can be improved from about 0.85 to 0.94 by increasing the primary nonequilibrium chamber temperature from about 750°K to about 2000°K. In the c^*-calculation the heat losses of the system are not taken into consideration, so that the c^*-data should be slightly higher than shown in Fig. 7.

4.3.3 Air to propellant ratio

The tests discussed in the previous section were run at a relative low air to propellant (a/p) ratio (lower than 6.7). Results

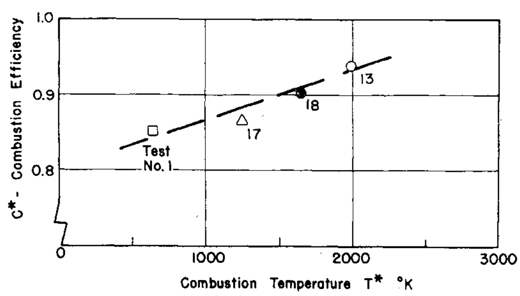

Fig. 7 Correlation of c^*-efficiency with nonequilibrium primary combustion temperature.

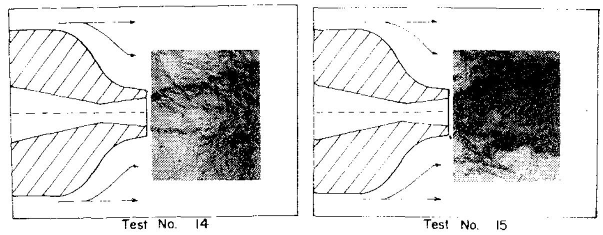

Fig. 8 Mixing and combustion characteristics at different air/propellant ratios. Test 14: 5.1, test 15: 11.8.

of tests at higher air to propellant ratios are shown in Figs. 8 and 9. Figure 8 shows a comparison of schlieren pictures made at a/p ratio of 5.1 and 11.8 with a nonequilibrium primary chamber temperature of about 1600°K for each test. The reaction of the gaseous species of the primary rocket (hydrogen) was more turbulent at higher a/p ratio, and a wider spread of the reaction zone at comparable distance was observed. This more intensive reaction characteristic was also noticed in the boron reaction behavior from a color picture (Fig. 9). The significant differences in the boron reaction at higher a/p ratio in comparison to lower a/p ratio but with the same primary rocket conditions were: 1) the boron reaction, apparently in connection with the air-hydrogen reaction, starts more intensively, causing an abrupt enlargement of the jet boundary and stronger spread of the visible jet boundary, and 2) the temperature increase of the particle cloud during the heating period was faster as indicated by the brilliant white-green combustion flame observed in the fourth window.

The tests at different a/p ratios were made with constant secondary nozzle area to keep the characteristic length L^*, the residence time in the afterburner, and the air inlet velocity constant. Thus, the increasing amount of airflow caused a higher secondary chamber pressure. The effect of increased pressure can be seen in the test data and must be considered when comparing the tests in Figs. 8 and 9. A separation of the influences (a/p ratios and afterburner pressure) on the boron reaction behavior was not possible. Preliminary tests were also run using a decreased secondary throat area. An improvement of the secondary combustion was observed. It could not be determined if this was due to the increased secondary chamber pressure or the increased residence time.

5. Conclusion and Discussion

It has been demonstrated that temperature of the boron particles in the exhaust from the primary rocket has a signifi-

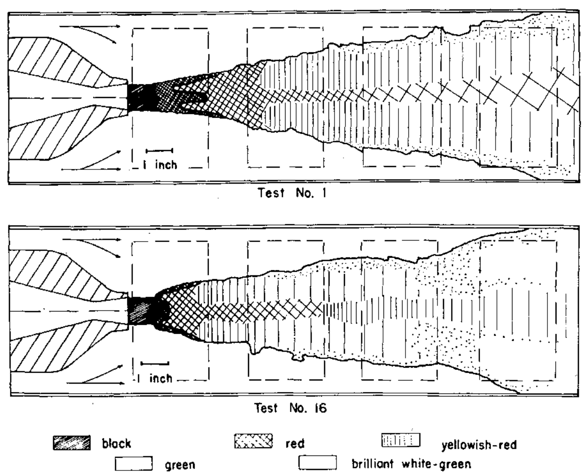

Fig. 9 Boron combustion behavior at different air/propellant ratios. Test 1: 6.7, test 16: 15.5.

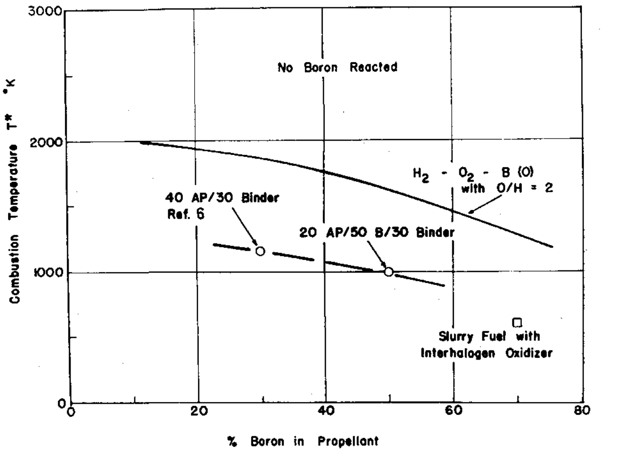

Fig. 10 Primary rocket T^* calculations for different propellants with boron.

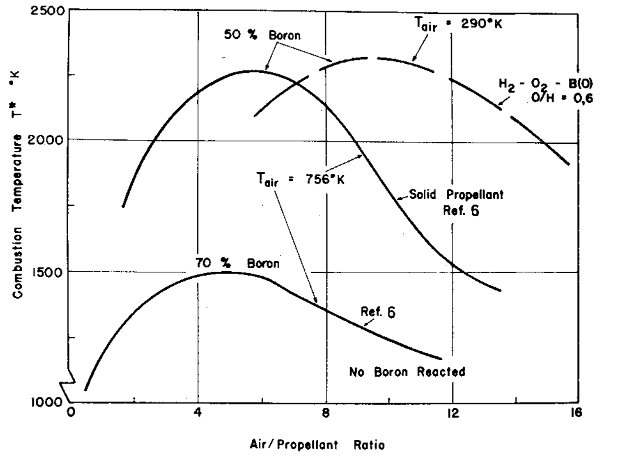

Fig. 11 Secondary chamber T^* calculations for different propellants with 290°K and 756°K air.

cant influence on the combustion of boron in the ingested air. To achieve highly efficient combustion the particle temperature should be as high as possible. Therefore, the combustion temperature of the nonmetallic propellant should be as high as possible. This requirement, of course, has to be optimized with other propellant and motor conditions in an air-augmented rocket: 1) good production behavior of heavily metallized propellants, 2) efficient, sustained burning, 3) positive expulsion characteristics from the primary rocket, 4) nonagglomeration of condensed-phase particles, and 5) high metal loading for maximum specific density impulse.

There are difficulties in transferring the results of the investigated hydrogen-oxygen-boron-air system to typical propellants for air-breathing application. A comparison should consider both thermodynamics and reaction kinetics. A comparison based on thermodynamic data (for example, the nonequilibrium primary and secondary temperatures) is possible, but the reaction kinetics aspects, especially the boron oxidation rate as a function of temperature and surrounding gas conditions, are not well enough understood to make exact comparisons for typical propellants for air-breathing application using the results of this paper. Therefore the following discussion has to be considered more as a speculation than as a result, and the data have to be viewed with the necessary limitations.

Two typical propellants for air-augmentation applications are solid propellants with 50% boron and liquid propellants with 70% boron in combination with an interhalogen oxidizer. The calculated nonequilibrium primary chamber temperatures of these propellants are compared in Fig. 10 with those calculated for the hydrogen-oxygen-boron system. The nonequilibrium temperature of this combination has been calculated for an oxygen-hydrogen mixture ratio of 2 (where high-efficiency boron combustion has been demonstrated) as a function of the boron concentration in the propellant. For this propellant combination the temperature dropped to about 1250°K as the boron weight was increased to 70%. In comparison to a 50% boron solid propellant and a 70% boron liquid propellant system (slurry), the nonequilibrium combustion temperature for the hydrogen-oxygen system was 500° to 700° higher.

The nonequilibrium temperature of the reaction of the gaseous species from the primary rocket with the ingested air (assuming boron as a heat sink) is shown in Fig. 11 as a function of the air to propellant ratio for the following propellant combinations: 1) hydrogen-oxygen-boron (O/H = 0.6; 50% boron) with 290°K air, 2) solid propellant (with 50% boron) with 756°K, and 3) propellant with 70% boron with 756°K air. The figure indicates that the maximum temperature for the propellant with 70% metal is 800°K less than the temperature of the hydrogen-oxygen-boron-air reaction. This combustion temperature T^* can be reached with the solid propellant (50% boron) using an air temperature of 756°K instead of 290°K.

On the basis of the calculated thermodynamic data, the 70% boron system does appear to fall considerably short of achieving T^* levels, in either the primary or the secondary chamber, for which high-efficiency combustion has been demonstrated with the hydrogen-oxygen-boron system. The solid propellant system with 50% boron is comparable (on the base of the calculated thermodynamic data) with the conditions of test 1 in this paper (T_{PRIMARY} ~1000°K; $T^*_{\text{SECONDARY}}$ ~2300°K). It was demonstrated that the combustion efficiency of this test could have been increased by a considerable factor by increasing the primary chamber nonequilibrium temperature.

With the available data it cannot be concluded that the typical liquid and solid propellants for air-breathing application would exhibit unsatisfactory efficiency without considering the kinetics of the boron reaction. It is known that the boron particles react when expelled from the primary chamber at temperatures calculated for the slurry fuel with interhalogen oxidizer. The oxidation rate is not normally rapid at these low temperatures, but depends on the surface conditions of the particle and the particle environment. As the gas composition surrounding the particle changes with each of the compared propellants, an adequate comparison of the results of the hydrogen-oxygen-boron system with the other propellants cannot be made at this time.

References

[1] Crump, J. E., private communication, Naval Weapons Center, China Lake, Calif., May 1968.

[2] Anderson, R., private communication, Consolidated Engineering Technology Corporation, Mountain View, Calif., June 1968.

[3] Talley, C. P., Woods, H. P., and Poplin, G., "Combustion of Elemental Boron," Progress Repts., Contract NOnr-1883 (00), 1960–1962, Texaco Experiment Inc., Richmond, Va.

[4] Prentice, J., private communication, Naval Weapons Center, China Lake, Calif., May 1968.

[5] Baumgartner, W. E., "Combustion of Thermogens in Solid Propellants," presented at the ICRPG/AIAA Solid Propulsion Conference, Washington, D.C., July 19–21, 1966.

[6] Cohen, N. S., "Combustion Considerations in Fuel-Rich Solid and Hybrid Propellant System in Air-Breathing Propulsion," AIAA Paper 68-96, New York, 1968.

[7] Dean, L. E. et al., "Ignition and Combustion of Aluminum in Small-Scale Liquid Rocket Engines," *Journal of Spacecraft and Rockets*, Vol. 2, No. 5, Sept.–Oct. 1965, p. 753–757.

[8] *Handbook of Chemistry and Physics*, Chemical Rubber Publ. Co., 1952–53.

[9] Crowe, C. T., "Dynamics of Two-Phase Flow in Rocket Nozzles," Final Rept., Contract Now 64-0506-C, Sept. 1965, United Technology Center, Sunnyvale, Calif.